EUROPEAN ORGANIZATION FOR NUCLEAR RESEARCH

Proposal to the ISOLDE and Neutron Time-of-Flight Committee

Emission Channeling with Short-Lived Isotopes: lattice location of impurities in semiconductors and oxides

25.9.2013

L.M.C. Pereira[1], L.M. Amorim[1], J.P. Araújo[4], V. Augustyns[1], K. Bharuth-Ram[6], E. Bosne[5], J.G. Correia[2], A. Costa[2], P. Miranda[7], D.J. Silva[4], M.R. da Silva[3], K. Temst[1], A. Vantomme[1], and U. Wahl[2]

(The EC-SLI collaboration)

1 Instituut voor Kern- en Stralingsfysica (IKS), KU Leuven, 3001 Leuven, Belgium
2 Centro de Ciências e Tecnologias Nucleares (C2TN), Instituto Superior Técnico, Universidade de Lisboa, 2686-953 Sacavém, Portugal
3 Centro de Física Nuclear da Universidade de Lisboa (CFNUL), 1649-003 Lisboa, Portugal
4 Departamento de Física, Universidade do Porto, 4169-007 Porto, Portugal
5 Departamento de Física, Universidade de Aveiro, 4169-007 Porto, Portugal
6 University of KwaZulu Natal, Durban 4041, South Africa
7 Departamento de Física, Universidad de Chile, Las Palmeras 3425, Santiago, Chile

Spokesperson: L.M.C. Pereira (lino.pereira@fys.kuleuven.be)
Local contact: J.G. Correia (Guilherme.Correia@cern.ch)

CERN-INTC-2013-031 / INTC-P-391
25/09/2013

Abstract

We propose to perform emission channeling lattice location experiments in a number of semiconductor and oxide systems of technological relevance:
- The lattice location of the transition metal probes ^{56}Mn ($t_{1/2}$=2.6 h), ^{59}Fe (45 d), ^{61}Co (1.6 h) and ^{65}Ni (2.5 h) is to be investigated in materials of interest as dilute magnetic semiconductors, such as GaMnAs, GaMnN, GaFeN, AlGaN, SiC, and in a number of oxides that are candidates for "single ion ferromagnetism", in particular $SrTiO_3$ and $LiNbO_3$.
- The topic of *p*-type doping of nitride semiconductors shall be addressed by studying the lattice sites of the acceptor dopants Mg and Be in GaN and AlN using the short-lived probes ^{27}Mg (9.5 min) and ^{11}Be (13.8 s). The aim is to reach a lattice location precision around 0.05 Å in order to provide critical tests for recent theoretical models which e.g. have predicted displacements of the Mg atom from the ideal substitutional Ga and Al sites of the order of 0.2-0.3 Å.
- The feasibility of using the short-lived positron emitter ^{11}C (20.4 min) for β^+ emission channeling experiments shall be tested. This part of the proposal will make use of newly developed beams of molecular $^{11}C^{16}O^+$ ions from molten salt targets.

Requested shifts: 30 shifts, (split into ~7 runs over 2-3 years)

1) Introduction

Emission channeling relies on implanting single crystals with radioactive probe atoms that decay by the emission of charged particles such as α, β^- or β^+ particles or conversion electrons, which, on their way out of the crystal, experience channeling or blocking effects along crystallographic axes and planes. The resulting anisotropic particle emission yield from the crystal depends in a characteristic way on the lattice sites occupied by the emitter atoms and is recorded with the aid of position sensitive detectors. In comparison to conventional lattice location techniques by means of ion beam channeling, e.g. Rutherford Backscattering/Channeling (RBS/C), the main benefits of emission channeling are a roughly four orders of magnitude higher efficiency and the ability to easily study also elements lighter than the host atoms. These facts allow performing detailed lattice location studies with very good statistical accuracy at low fluences of implanted probe atoms, usually as a function of implantation or annealing temperature of the very same sample, which is not feasible by other methods.

2) Short status report on previous EC-SLI experiment IS453

Our publications resulting still from IS453 "Emission channeling lattice location experiments with short-lived isotopes" after the year 2010 (the date of its addendum) are listed in section 6a) [1-18].
Following its commissioning in 2007, the EC-SLI on-line emission channeling chamber was in 2008 upgraded with a closed-cycle He refrigerator which allows cooling the sample to 50 K, and in 2011 with a high-precision 3-axis goniometer with *x*,*y*,*z* translation stage from the company Panmure. The current status of the on-line chamber has been documented in a recent publication in Rev. Sci. Instr. [10].
In 2012 we commissioned a new Small Implantation Chamber (SIC) which is mounted in front of our on-line setup at GHM. The SIC allows in particular to make parallel collections of long-lived isotopes in this beamline while other users take radionuclides with lower masses in GLM or the central beamline, thus greatly increasing the opportunities for parallel operation of GPS.
The following four PhD students are currently working within the scope of this proposal:
- Lígia Amorim (since Jan. 2010) on "Lattice location studies of implanted Mg in the III-nitride semiconductors GaN, AlN and InN", IKS, KU Leuven;
- Daniel Silva (since Jan. 2011) on "Lattice location of transition metals in Si by means of high-resolution emission channeling", Faculdade de Ciências da Universidade do Porto;
- Ângelo Costa (since Nov. 2012) on "Ion implantation doping of SiC", Instituto Superior Técnico, Universidade de Lisboa;
- Valérie Augustyns (since Sept. 2013), tentative topic of thesis: "Lattice location experiments of transition-metal doped oxides", IKS, KU Leuven.

3) Physics cases

3a) Transition metals as magnetic dopants in dilute magnetic semiconductors and oxides

In a dilute magnetic semiconductor (DMS), magnetic ions are introduced in an otherwise non-magnetic semiconductor. The discovery of a DMS which is ferromagnetic above room temperature is regarded as the 'holy grail' of semiconductor spintronics [19-21]. Despite the success of narrow-gap DMSs such as Mn-doped GaAs, where ferromagnetism and semiconducting behaviour do co-exist, producing rich spintronic phenomena [20,21], the maximum Curie (ordering) temperatures (T_C) remain well below room temperature (< 200 K) [21]. Although higher T_C have been predicted and reported for wide-gap DMSs such as transition-metal doped ZnO, GaN, and SiC, there is yet no consensus that intrinsic ferromagnetism is established in such materials [13,21-23].

For Mn-doped GaAs, the model narrow-gap DMS, it is well established that, whereas the majority of Mn ions substitute for Ga (Mn_{Ga}), a few % may occupy interstitial sites [24]. While Mn_{Ga} provides both the localized magnetic moment and the itinerant hole that mediates the magnetic coupling, interstitial Mn_i acts as a compensating defect, both electrically and magnetically. Consequently, although a minority

fraction, Mn_i plays a key role in determining the magneto-electric properties of Mn-doped GaAs, in particular T_C [25]. Within the scope of IS453, we addressed key aspects which were still poorly understood. For the first time, we directly identified the Mn_i interstitial site as the tetrahedral interstitial with As nearest neighbors (T_{As}), contrary to a prevailing belief based on indirect experimental evidence that Mn_i prefers T_{Ga} [5,8]. More importantly, we showed that in the low concentration regime (<0.05 at. % Mn) Mn_i has a much higher thermal stability than that previously reported for the high concentration regime (>1 at. % Mn), raising fundamental questions regarding the current interpretation of the increase in T_C upon thermal annealing [5,8]. In the current proposal we aim to address these questions further, by extending the narrow-gap studies into the ferromagnetic high doping regime. In 2012, we successfully tested the feasibility of such experiments, using as samples thin films of $Ga_{.95}Mn_{.05}As$ (doped with stable ^{55}Mn during growth by molecular beam epitaxy) which were implanted at ISOLDE with radioactive ^{56}Mn (to a fluence of the order of 10^{12} at./cm^2, i.e. orders of magnitude lower than the 5% of stable Mn incorporated during growth).

Compared to Mn-doped GaAs, wide-gap DMSs (in partciular TM-doped ZnO and GaN) are strikingly different. For instance, for comparatively ionic compounds it is generally accepted that the TM dopants (Mn, Fe, Co, Ni) occupy only cation sites (TM_{Zn} in ZnO and TM_{Ga} in GaN). Regarding the magnetic behavior of these systems, a 13 year long debate continues to divide the magnetism community between those who report intrinsic ferromagnetism above room temperature and those who argue that such reports are based on experimental artifacts [5,20]. Within the scope of IS453 we carried out extensive emission channeling studies on the lattice location of ^{56}Mn, ^{59}Fe, ^{61}Co and ^{65}Ni in ZnO and GaN [6,9,11,13,14,18]. Contrary to the general belief that TMs occupy only cation substitutional sites, we have shown that, among the eight studied combinations of TM dopants and hosts, five show significant fractions (~20%) of anion substitution (Mn, Co and Ni on O sites in ZnO [6,11,18], and Mn and Co on N sites in GaN [9,14,18]). These findings, obtained in the very low concentration regime (<0.05 at. %) have profound implications on the general understanding of lattice site preference of impurities in compound semiconductors. In the current proposal, we also aim at extending these studies to selected samples in the high doping regime, e.g. ^{56}Mn in $Ga_{1-x}Mn_xN$. In addition, we will investigate the effect of increasing the bandgap of the host semiconductor, from 3.4 eV for GaN to 6.2 eV for AlN, and intermediate values for (Al,Ga)N alloys. On the other hand, we plan to also study TMs in the covalently bonded wide gap semiconductors 3C-SiC and 6H-SiC.

Within the scope of IS453 we have also addressed the above-mentioned debate on the origin of the often reported room temperature ferromagnetism in wide-gap DMSs. To do so, we selected the Fe-doped ZnO system, which shows pure cation substitution, and carried out a detailed study of the local structure and magnetism, combining ^{59}Fe emission channeling with several methods of structural and magnetic characterization [13]. These studies were performed on the high doping regime (0.7-7 at. % Fe), typical for the often reported ferromagnetism in wide-gap DMSs, by pre-implanting ZnO single crystals with stable ^{56}Fe to fluences between 10^{15} and 10^{16} at./cm^2. We have demonstrated that: (i) isolated Fe_{Zn} behave as localized paramagnetic moments down to 2 K, irrespective of the Fe concentration and the density of beam-induced defects; (ii) with increasing local concentration of Fe_{Zn}, strong nearest-cation-neighbor antiferromagnetic interactions favour the antiparallel alignment of the Fe moments. These findings strongly support the notion that TMs in wide-gap semiconductors such as GaN and ZnO do not order ferromagnetically [21]. In the current proposal we aim at applying a similar methodology to a new paradigm of room temperature ferromagnetism in DMS, which we introduce in the next paragraph.

Despite the extensive research on narrow-gap and wide-gap DMSs, the main goal of the field, i.e. to reach room temperature ferromagnetism, remains to be achieved. In narrow-gap DMSs such as Mn-doped GaAs, where the ferromagnetic order is mediated by free carrier holes, there may exist a fundamental limit to the achievable T_C [21]. In contrast, the fundamental issue with wide-gap DMSs such as TM-doped ZnO and GaN is the lack of a demonstrated mechanism of magnetic interaction which is sufficiently strong and long-ranged to produce high-temperature magnetic order in dilute magnetic compounds [21]. There is, however, an alternative new picture in which ferromagnetic order can emerge from single-ion

phenomena, in the absence of magnetic interaction [26,27]. Indeed, Prof. Caroline Ross' group (MIT, USA) has recently reported on single-ion (anisotropy-driven) ferromagnetic order above room temperature in Fe- and Co-doped $SrTiO_3$ grown by pulsed laser deposition (PLD) [28]. This exciting new paradigm has so far received very little attention by the DMS community, remaining virtually unexplored. Using a combination of magnetic and structural characterization techniques we have already carried out extensive studies on Fe- and Co-doped $SrTiO_3$, prepared by ion implantation (up to fluences of the order of 10^{16} at./cm^2, i.e. few at. %). SQUID magnetometry shows ferromagnetic behavior well above room temperature, which is activated by high temperature annealing in vacuum at 700-900ºC, de-activated by annealing in air and activated again by annealing in vacuum. A unique combination of ^{59}Fe emission channeling [29] and extended X-ray absorption fine structure (EXAFS) measurements shows that the Fe impurities substitute for Ti in the $SrTiO_3$ perovskite lattice. Conversion electron Mössbauer spectroscopy (CEMS) and synchrotron radiation X-ray diffraction (SR-XRD) have further excluded the presence of ferromagnetic secondary phases (metallic Fe, Fe_nO_m, etc), showing that the observed ferromagnetism is indeed an intrinsic property of $Sr(Ti,Fe)O_3$. In particular, correlating the data from the different techniques (EC, SQUID and CEMS) we can infer that there are in fact two distinct Fe fractions: Fe ions which occupy ideal Ti sites and are paramagnetic, and the ferromagnetic Fe, which is displaced towards the O nearest neighbour by 0.6 Å, due to the formation of complexes between Fe_{Ti} impurities and O vacancies (V_O), as depicted in Fig. 1.

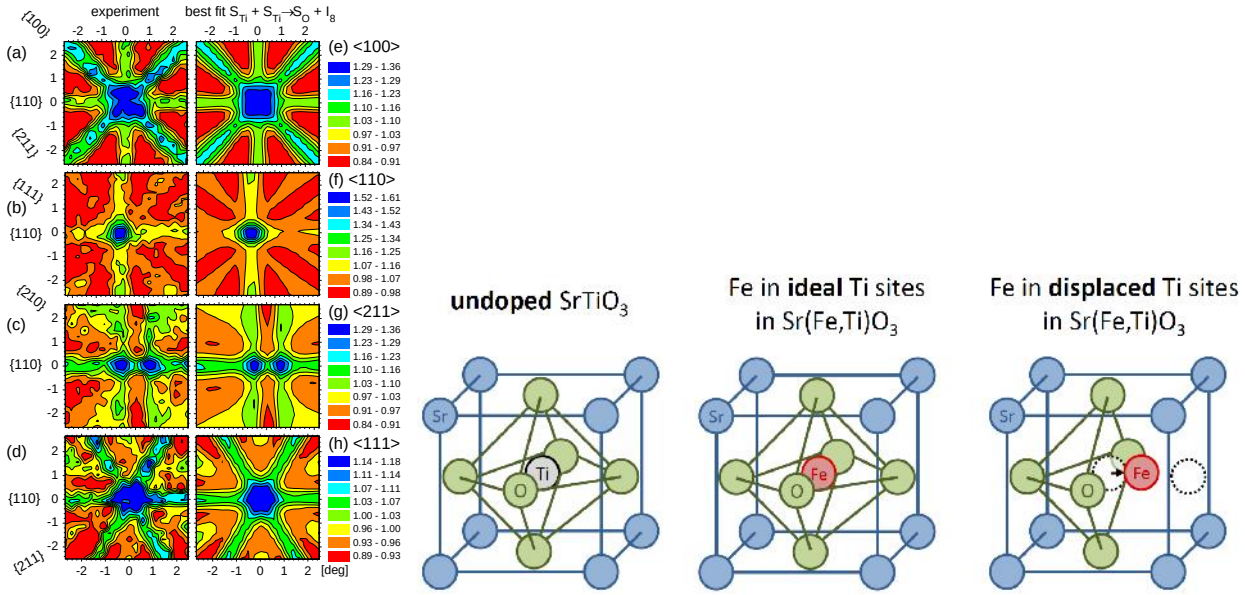

Figure 1: Left: Angular distributions of β^- particles emitted from ^{59}Fe in $SrTiO_3$ around the (a) <100>, (b) <110>, (c) <211> and (d) <111> directions following room temperature implantation and vacuum annealing for 10 min at 750ºC. The best fits of the simulated patterns are shown in Fig.1 (e)-(h) and correspond to 18% of Fe_{Ti} and 44% of Fe_{Ti}-V_O. From Ref. [29]. Right: structure of undoped $SrTiO_3$, and Fe on Fe_{Ti} and Fe_{Ti}-V_O.

These findings suggest that the local symmetry-breaking (responsible for the single-ion magnetic order) does not originate from Jahn-Teller distortion (tetrahedral expansion/contraction), as initially described by the MIT group [26-28], but from the presence of V_O and resulting static displacement of the Fe ions in Fe_{Ti}–V_O complexes. Recently, the MIT group and the Leuven group have joined efforts in pursuing a general understanding of this new phenomenon of single-ion ferromagnetism. This will entail a wide research program on the local structure and magnetism of TM-doped oxides. In addition to $SrTiO_3$, other oxides will be selected based on the following criteria: (i) possessing cation sites with octahedral coordination, a fundamental ingredient for the phenomenon in question, (ii) the ability to be properly

annealed after high fluence implantation; (iii) displaying other properties of interest to be combined with the ferromagnetic order. An example of such oxides is $LiNbO_3$, which satisfies all three conditions, being a commonly used ferroelectric. Regarding the TM dopant elements, we will focus on ^{56}Mn, ^{61}Co, and ^{65}Ni, and ^{59}Fe. As illustrated by the Fe-doped $SrTiO_3$ example above, emission channeling plays a crucial role in these studies. It is the only experimental technique allowing for unambiguous, quantitative, multisite lattice location, all of which are indispensible aspects for the physics in question. Although originally motivated by the DMS field, this phenomenon of single-ion ferromagnetism in TM-doped oxides goes far beyond it. To some extent, it is on its own a new topic of condensed matter physics: a fundamentally new type of ferromagnetism which does not rely on magnetic interaction, contrary to all other known mechanisms of ferromagnetic order. In addition, this phenomenon has promising ramifications in other contemporary topics of condensed matter physics. For example, it is a potential route for a new type of multiferroicity, if single-ion ferromagnetism is induced in ferroelectric oxides such as $LiNbO_3$, as mentioned above. Moreover, ferromagnetic defect complexes such as Fe_{Ti}-V_O in $SrTiO_3$ are an ideal candidate for what has been recently coined as quantum spintronics [30], as they are likely to have longer spin-coherence compared to the commonly investigated paramagnetic defects (V_{Si}-V_C divancies in SiC and N-V_C complexes in diamond [30]).

Proposed experiments: We intend to use shortlived ^{56}Mn ($t_{1/2}$=2.6 h), ^{61}Co (1.6 h) and ^{65}Ni (2.5 h) for on-line and long-lived ^{59}Fe (45 d) for off-line experiments. While ^{56}Mn and ^{65}Ni are directly obtained at ISOLDE from RILIS laser ion sources, ^{61}Co is implanted via the precursor isotope ^{61}Mn, exploiting the decay chain ^{61}Mn (0.71 s) → ^{61}Fe (6 min) → ^{61}Co, and ^{59}Fe is implanted via the precursor isotope ^{59}Mn (4.6 s) → ^{59}Fe.

Regarding the experiments on $Ga_{1-x}Mn_xAs$, our first goal is to determine the activation energy for diffusion of interstitial and substitutional Mn as a function of Mn concentration (x = 0.01–0.2). These studies will consist of room temperature implantation of short-lived ^{56}Mn into $Ga_{1-x}Mn_xAs$ thin films grown by molecular beam epitaxy, followed by measurements as a function of annealing temperature between 100 and 900ºC. The second goal is to determine the migration barrier between two adjacent T sites, i.e. from a metastable T_{Ga} to a stable T_{As} site [24]. These experiments will require low temperature implantation of ^{56}Mn (down to 50 K), whereby we are likely to 'freeze' ^{56}Mn ions in T_{Ga} sites. By performing emission channeling measurements as a function of temperature up to 300 K, we will be able to monitor the T_{Ga} fraction being converted to T_{As} and thereby determine the $T_{Ga} \rightarrow T_{As}$ migration barrier.

For wide-gap DMSs, our goal is to advance the understanding of the puzzling anion substitution found in some of the TM-host combinations. To do so, we will extend these studies to the high doping regime, focusing on two selected systems: Mn-doped GaN, for which we have observed minority N substitution, and Fe-doped GaN for which we observed pure Ga substitution. The experiments will consist of emission channeling measurements of $Ga_{1-x}Mn_xN$, $(Al,Ga)_{1-x}Mn_xN$ and $Ga_{1-x}Fe_xN$ thin films (grown by metalorganic vapour phase epitaxy, with x = 0.01–0.10), implanted at room temperature with radioactive ^{56}Mn and ^{59}Fe, as a function of annealing temperature between 300 and 900ºC. These ^{56}Mn and ^{59}Fe emission channeling experiments will be complemented by ^{57}Mn → ^{57}Fe emission Möessbauer experiments (cf. proposal presented to the INTC.)

Regarding the experiments on TM-doped oxides, our aim for an initial 2-3 year period is to comprehensively establish the lattice location of Mn, Fe, Co and Ni in $SrTiO_3$, $LiNbO_3$ and potentially other oxides. We will give priority to ^{56}Mn and ^{59}Fe, both obtained from RILIS Mn beams (contrary to ^{65}Ni which requires dedicated RILIS Ni beams) and which, based on our experience, allow for a more efficient use of the beam time compared to ^{61}Co (due to lower yields of ^{61}Mn and loss of ^{61}Co activity during the decay-chain waiting time). These experiments will consist of emission channeling measurements (as a function of annealing temperature between 300 and 900ºC) after implantation of the radioactive probes (up to fluences of the order of 10^{12} at./cm^2) into pure oxides and samples which have been pre-implanted with stable TMs (up to fluences of the order of 10^{16} at./cm^2). Due to the poor reproducibility of the 60 kV operation at ISOLDE, the pre-implants will consist of multi-energy implantations which allow for a nearly flat depth profile of the pre-implanted ions. This will circumvent the otherwise necessary match of the energy chosen for the pre-implantation and the acceleration energy

used during the radioactive run. The ^{59}Fe emission channeling experiments will be complemented by ^{57}Co → ^{57}Fe emission Mössbauer experiments (IS501).
All the emission channeling studies described above are part of a wide research program of the IKS Leuven group on dilute magnetic semiconductors, involving several other large-scale-facility methods: synchrotron radiation techniques such as extended X-ray absorption fine structure, X-ray magnetic circular dichroism and nuclear resonant scattering; neutron scattering techniques such as polarized neutron reflectivity.

3b) Lattice location of Mg and Be in nitride semiconductors

The remark given in the motivation of our original proposal from 2006, that "Mg represents the only feasible *p*-type dopant in the technologically important wide band gap semiconductor GaN" remains valid. All applications of GaN involving *pn*-junctions such as blue or white LEDs, blue lasers and high-frequency power diodes still rely on Mg doping. In addition, we had stated in our Jan. 2010 addendum: "Moreover, recent experimental evidence [31] indicates that there exist two types of Mg acceptor centers in GaN, although no detailed structural models have been proposed in order to distinguish them." This situation has meanwhile changed with the publication of new, detailed microscopic models for the Mg_{Ga} acceptor in GaN and AlN. In particular, Lany and Zunger [32] have presented a model which proposes that for the neutral, i.e. unionized acceptor Mg_{Ga}^{0} one of the basal Mg-N bonds is elongated by about 10%, which leads to a ~0.20 Å basal displacement of the Mg atom from the ideal substitutional Ga site. More recently, Lyons et al [33] have come forward with a similar theoretical model, which also suggests that Mg_{Ga}^{0} induces a "large local lattice distortion" characterized by an elongation of one of the Mg-N bonds by 15% (0.29 Å). Naturally, our aim is to test the validity of these models by means of on-line lattice location experiments using ^{27}Mg (9.5 min).

We obtained beam time for ^{27}Mg in 2009 (from a SiC target), 2010 (SiC target), 2011 (Ti target) and 2012 (UC_x target). However, as is known by now, only the Ti-W RILIS Mg target and ion source combination can provide clean ^{27}Mg without contamination of ^{27}Al (stable) and ^{27}Na (300 ms). In that respect, the 2009 and 2010 beam times were plagued by the fact that the target and line had to be run under relatively cool conditions in order to suppress ^{27}Al, which also considerably decreased the yields of ^{27}Mg (roughly by a factor 15–20). Although in 2011 the contamination problems could be solved after development of the Ti target, it was impossible to schedule such a target in 2012 following the breakdown of GPS and the resulting emergency schedule which relied on the use of HRS only. As substitute we had to share a UC_x target with other users. While the ^{27}Al contamination from the UC_x, target was considerably less than from SiC, ^{27}Na turned out to be such a problem that meaningful data could only be obtained once the sample had been loaded ~30 min with ^{27}Mg and the beam turned off during the actual measurement. This procedure, however, is only around 1/4 as efficient as real on-line experiments where we implant and measure at the same time, as is possible using a Ti target.

Our emission channeling measurements of ^{27}Mg in GaN and AlN were the first direct lattice location experiments of Mg in nitride semiconductors. They clearly showed that the large majority of ion implanted Mg is incorporated on Ga or Al sites. However, following room temperature implantation also interstitial fractions of 23% (AlN, Fig. 2, [17]) and 26% (GaN) near the octahedral O sites could be identified. Implantation temperatures above 400°C in AlN or above 600°C in GaN resulted in complete conversion of the interstitial fraction to substitutional Al or Ga sites, from which we were able to estimate the activation energy for the migration of interstitial Mg to be be around 1.1-1.7 eV in AlN and 1.6-2.5 eV in GaN. We found possible displacements of ^{27}Mg from ideal Al or Ga sites to be not larger than 0.1 Å (thus not confirming the theoretical models mentioned above) but the interstitial positions could be determined only with an accuracy of ~0.3 Å.

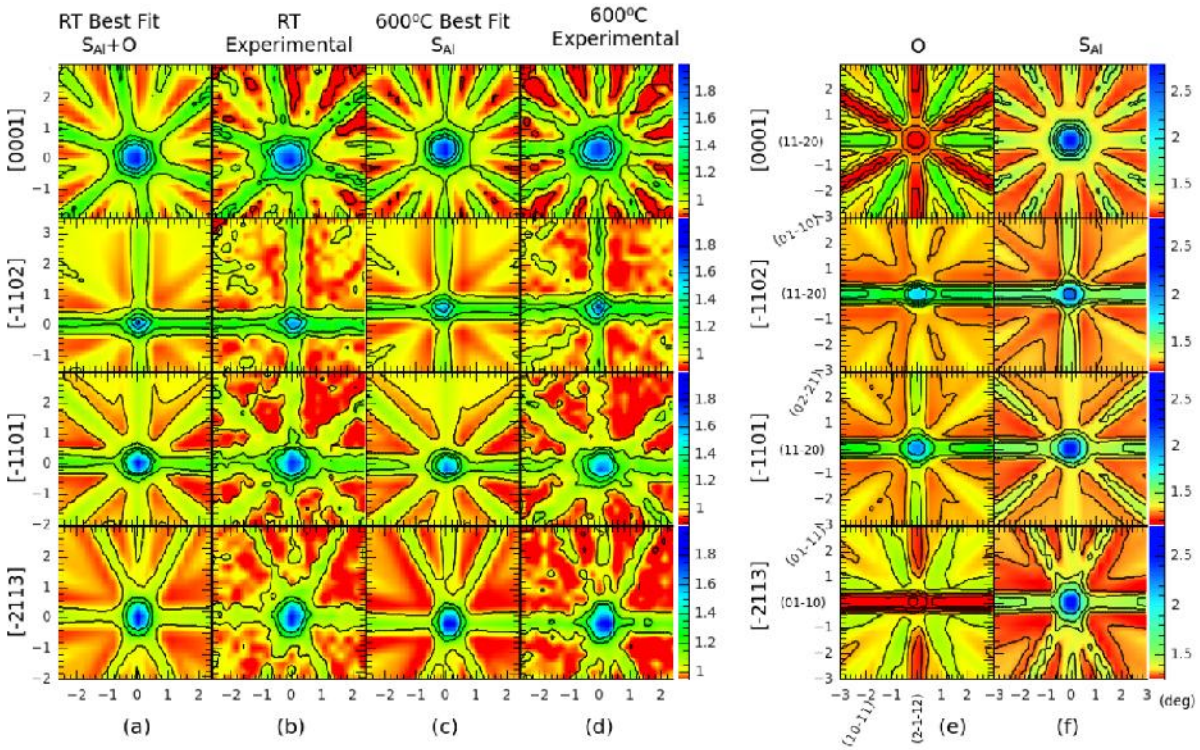

Figure 2: Columns **(e)** and **(f)** are the theoretical patterns for 100% of ^{27}Mg on octahedral interstitial sites O and substitutional Al sites S_{Al} in AlN. Columns **(a)** and **(c)** are experimental β^- emission channeling patterns from ^{27}Mg in AlN during RT and 600°C implantation, respectively. Columns **(b)** and **(d)** are the respective best fits, which for RT implantation correspond to 76% of ^{27}Mg emitter atoms on S_{Al} and 23% near interstitial O sites, while for 600°C implantation only emitter atoms on S_{Al} sites are found, but with a fraction of 97%. From Ref. [17].

In the current proposal, we aim at high angular resolution studies which should allow to better characterize the exact location of substitutional and interstitial ^{27}Mg in AlN and GaN and the thermally activated lattice site change. We are confident that the precision and accuracy of lattice location can be further improved, reaching even below the rms vibrations of the lattice atoms, around 0.06 Å in GaN. The high-resolution studies, however, require that the distance between sample and position-sensitive detector is doubled, which reduces the solid angle and hence also the count rate in the experiments by a factor of 4, requiring therefore ^{27}Mg beams of high yield. Such experiments should be perfectly possible using Ti targets.

Our second goal are ^{27}Mg experiments at temperatures down to 50 K. Implantation at low temperatures is likely to increase the interstitial fraction of Mg: if the mobility of the created Ga and Al vacancies V_{Ga} and V_{Al} can be suppressed by cooling, the combination of V_{Ga} with interstitial Mg is hindered. Such type of experiments may hence also give crucial information about the mobility of the cation vacancies in III-nitrides. Absence of ^{27}Al is particularly relevant in this case, since at low temperatures the semiconductors are more sensitive to the creation of radiation damage. At a later stage one may also consider EC-SLI experiments in hydrogenated nitride samples since it is well-known that H passivates the acceptor action of Mg in GaN, or experiments in narrow gap III-Vs such as GaAs.

In 2012 we were able to demonstrate in parasitic trials the feasibility of lattice location experiments with ^{11}Be (13.8 s) in GaN (Fig. 3). EC-SLI experiments using ^{11}Be are particularly challenging due to the high β^- endpoint energy of this isotope (11.5 MeV) which causes very narrow channeling effects. We hence ask now for beam as main users in order to also perform full EC studies with ^{11}Be as a function of implantation temperature in AlN and GaN. Particularly in the case of AlN this will be of relevance since there is an on-going debate which element might be the best-suited acceptor for this extreme wide band gap semiconductor, and Be_{Al} represents one candidate.

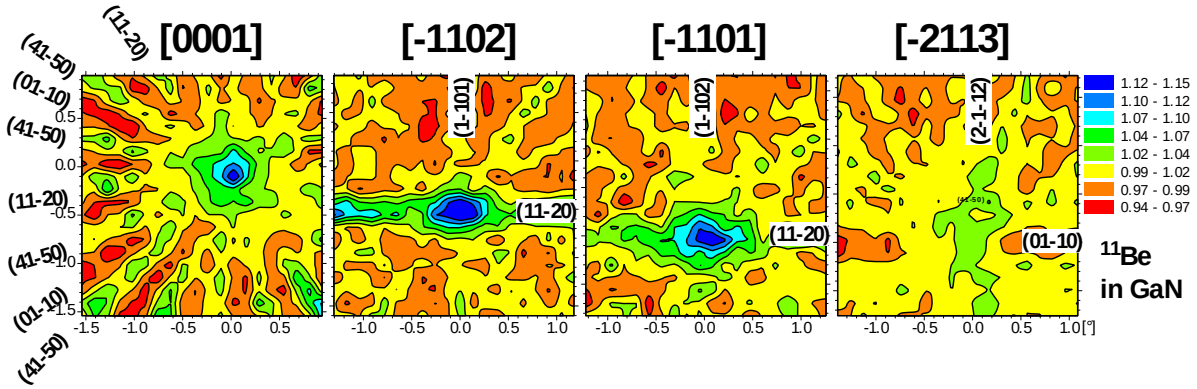

Figure 3: Emission channeling patterns from ^{11}Be in GaN, measured during room temperature implantation with high angular resolution. The fact that the set of (01−10) planes exhibits blocking effects while (11−20) and (41−50) planes show channeling effects is strong evidence that, besides substitutional Ga sites, a large fraction of Be is located near octahedral interstitial O sites.

Proposed experiments: We propose to continue the studies of the lattice sites of implanted short-lived ^{27}Mg ($t_{1/2}$=9.46 min) and ^{11}Be (13.8 s) in the nitride semiconductors GaN and AlN with high angular resolution and extend them also to low-temperature implantation. At a later stage, also ^{27}Mg and ^{11}Be in other III-V semiconductors, may be investigated. For ^{27}Mg, the proposed experiments should make use of Ti-W targets with RILIS Mg, which has proven to be the only target/ion source combination free of ^{27}Al and ^{27}Na contaminations.

4) Trial run of ^{11}C

Under materials science aspects, carbon is an important impurity in many technologically relevant crystalline solids, e.g. in semiconductors as a dopant or contaminant, or in metals, especially steel, as a structural component. Carbon implantation, followed by high-temperature thermal annealing, has recently attracted considerable attention since it allows to form graphene layers on top of Ni [34]. As a contaminant in Si, the typical concentration of C impurities (~10^{16}–10^{17} cm^{-3} in CZ-Si, ~10^{15} cm^{-3} in FZ-Si) is only surpassed by oxygen (usually an order of magnitude higher than C). Yet the actual knowledge on its possible lattice sites is surprisingly not very detailed. It is commonly assumed that C in Si is located mostly substitutional, but optical and DLTS spectroscopy as well as theory also point at the existence of interstitial C and C complexes [35,36]. Among various possible interstitial sites, the so-called <100> dumbbell (or SP <100>) is considered most stable [37]. In GaAs, the electrical activity of C depends on whether it replaces Ga (donor action) or As (acceptor action). The fact that C-doped GaAs is *p*-type then suggests that C mostly substitutes As, but this is by no means clear. It has been reported that C implanted in GaAs initially occupies interstitial sites and is promoted to substitutional sites by annealing at 500°C, although the exact nature of both sites was never resolved [38]. Another example is the understanding of implantation damage annealing in the two wide band gap semiconductors SiC and diamond, for which purpose information on possible lattice sites of C is obviously crucial. In all these cases, experiments with the emission channeling method, which is well able to distinguish between different types of interstitial sites and also e.g. between the two sublattices of Ga and As in GaAs, are certainly to reveal new insights. The most suitable probe atom for EC experiments with carbon is ^{11}C (20.39 min), which is a β^+ emitter with 961 keV endpoint energy. This isotope has recently become available at ISOLDE with high yields of ~7×10^8 atoms/μC as $^{11}C^{16}O^+$ molecular ion from new molten salt targets [Th. Stora, private communication].

Apart from the materials science interest, the use of ^{11}C as an EC probe is also very intriguing under the fundamental aspect of further development of the technique. Due to the fact that pure β^+ emitting isotopes are much less common in nature than β^- or conversion electron emitters, the simulation and quantitative analysis of positron emission channeling and blocking has never been investigated in detail. However, we

have already theoretical results that indicate that a simple inversion of the interaction potential is probably sufficient to allow accurate simulation of positron channeling by means of our *manybeam* code (Fig 4).

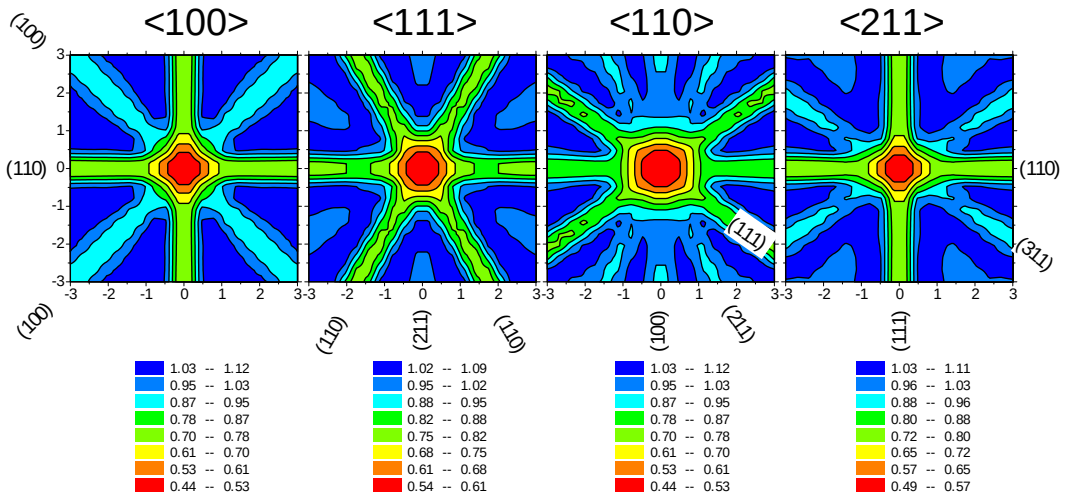

Figure 4: Expected positron blocking patterns from substitutional ^{11}C in Si at room temperature for $^{11}C^{16}O^{+}$ implantation with 50 keV. The *manybeam* calculation used potentials which were obtained by inverting the Doyle-Turner potentials for electrons and increasing the number of beams used.

We hence ask for 3 test shifts for the ^{11}C isotope. If successful, the implementation of positron emission channeling with ^{11}C, followed by an appropriate materials science program, would provide attractive options for several PhD topics.

Proposed experiments: 3 test shifts of ^{11}C are requested in order to test its feasibility for β^{+} emission channeling lattice location experiments. First materials to be studied will be comparatively simple systems such as Si, GaAs, 3C-SiC, or diamond.

5) Summary of requested shifts:

We request a total of 30 shifts over a period of 2-3 years for the isotopes specified below in Table 1. All requested targets (except molten salt) are standard ISOLDE targets and most beam times can hence be shared with other users. While the yields of most isotopes are known from previous runs, the achieved yield of $^{11}C^{16}O^{+}$ has been obtained from recent information by Th. Stora. Our previous experiment IS453 has 4.5 shifts left, mostly due to the fact that we only got much less ^{27}Mg beam time in 2012 (2.5 shifts) than actually requested (8 shifts). The current beam request is based on the assumption that we close IS453 and its remaining shifts will not be used.

The extensive program that we have foreseen for off-line experiments using the long-lived ^{59}Fe during the next 2 years would in fact require around 10-15 shifts of this isotope. However, here we are planning to perform a large part of these implantations in parallel by means of using the Small Implantation Chamber SIC on GHM for mass 59 while the main user will be Mössbauer experiments in GLM with mass 57.

As was mentioned already, the EC-SLI on-line emission channeling setup is currently installed at the GHM beamline of GPS. Since this position provides much more favourable conditions with respect to the required collimation of the ISOLDE beam than the LA1 or LA2 beam lines used previously, we ask to keep it. For implantation of the longer-lived isotopes, we will use the standard solid-state physics implantation chamber on GLM and our new Small Implantation Chamber (SIC) on GHM. The corresponding measurements will be done off-line with the emission channeling setups located in the new ISOLDE laboratory for radioactive off-line experiments (building 508).

Table 1: Requested isotopes, number of shifts, targets, ion sources and minimum yield requirements.

isotope	number of shifts	target	ion source	minimum yield [atoms/s/μA]
^{56}Mn (2.6 h)	4	UC_x-W	RILIS Mn	5×10^7
^{61}Mn (4.6 s) $\rightarrow$ ^{61}Fe (6 min) $\rightarrow$ ^{61}Co (1.6 h)	1	UC_x-W	RILIS Mn	2×10^6
^{59}Mn (0.71 s) $\rightarrow$ ^{59}Fe (45 d)	1	UC_x-W	RILIS Mn	10^8
^{65}Ni (2.5 h)	3	UC_x-W	RILIS Ni	5×10^7
^{27}Mg (9.5 min)	12	Ti-W	RILIS Mg	1×10^7
^{11}Be (13.8 s)	6	UC_x-W or Ta-W	RILIS Be	6×10^6
^{11}C (20 min) as $^{11}C^{16}O^+$ molecule	3	Molten salt, NaF-LiF eutectic	VD5 plasma	5×10^7 (achieved 7×10^8)
	Total: 30			

6) Publications and References

6a) Publications since 2010 related to our previous experiment IS453:

[1] A. Vantomme, U. Wahl, and B. De Vries: "Lattice location of rare earth impurities in III-nitrides", Topics in Applied Physics 124 (2010) 55-98.

[2] S. Decoster, S. Cottenier, U. Wahl, J.G. Correia, and A. Vantomme: "Lattice location of ion implanted Sn and Sn-related defects in Ge", Phys. Rev. B 81 (2010) 155204/1-6, CERN-OPEN-2013-007.

[3] S. Decoster, S. Cottenier, U. Wahl, J.G. Correia, L.M.C. Pereira, M.R. Da Silva, and A. Vantomme: "Diluted manganese on the bond-centered site in germanium", Appl. Phys. Lett. 97 (2010) 151914/1-3, CERN-OPEN-2013-008.

[4] U. Wahl, J.G. Correia, S. Decoster, and T. Mendonça: "Lattice location of the group V elements Sb, As, and P in ZnO", Proc. SPIE (2010) 7603K/1-15.

[5] L.M.C. Pereira, U. Wahl, J.G. Correia, S. Decoster, M.R. da Silva, J.P. Araújo, and A. Vantomme: "Direct identification of interstitial Mn in heavily *p*-type doped GaAs and evidence of its high thermal stability", Appl. Phys. Lett. 98 (2011) 201905/1-3, CERN-OPEN-2013-009.

[6] L.M.C. Pereira, U. Wahl, S. Decoster, J.G. Correia, L.M. Amorim, M.R. da Silva, J.P. Araújo, and A. Vantomme: "Mixed Zn and O substitution of Co and Mn in ZnO", Phys. Rev.B 84 (2011) 125204/1-6.

[7] S. Decoster, U. Wahl, S. Cottenier, J.G. Correia, T. Mendonça, L.M. Amorim, L.M.C. Pereira, and A. Vantomme: "Lattice position and thermal stability of diluted As in Ge", J. Appl. Phys. 111 (2012) 053528/1-7, CERN-OPEN-2013-011.

[8] L.M.C. Pereira, U. Wahl, S. Decoster, J.G. Correia, M.R. da Silva, A. Vantomme, and J.P. Araújo: "Stability and diffusion of interstitial and substitutional Mn in GaAs of different doping types", Phys. Rev. B 86 (2012) 125206/1-8, CERN-OPEN-2013-012.

[9] L.M.C. Pereira, U. Wahl, S. Decoster, J.G. Correia, M.R. da Silva, A. Vantomme, and J.P. Araújo: "Evidence of N substitution by Mn in wurtzite GaN", Phys. Rev. B 86 (2012) 195202/1-4, CERN-OPEN-2013-013.

[10] M.R. Silva, U. Wahl, J.G. Correia, L.M. Amorim, and L.M.C Pereira: "A Versatile Apparatus for On-line Emission Channeling Experiments", Rev. Sci. Instr. 84 (2013) 073506/1-8.

[11] L.M.C. Pereira, U. Wahl, J. G. Correia, L.M. Amorim, D.J. Silva, E. Bosne, S. Decoster, M.R. da Silva, K. Temst, and A. Vantomme: "Minority anion substitution by Ni in ZnO", Appl. Phys. Lett. 103 (2013) 091905.

[12] D.J. Silva, U. Wahl, J.G. Correia, and J.P. Araújo: "Influence of n^+ and p^+ doping on the lattice sites of Fe in Si", J. Appl. Phys. 114 (2013) 103503/1-9.

[13] L.M.C. Pereira, U. Wahl, J.G. Correia, M.J. Van Bael, S. Decoster, K. Temst, A. Vantomme, and J.P. Araújo "Paramagnetism and antiferromagnetic interactions in phase-pure Fe-implanted ZnO", J. Phys.: Condensed Matter 25 (2013) 416001/1-15.

[14] L.M.C. Pereira, U. Wahl, J.G. Correia, L.M. Amorim, D.J. Silva, S. Decoster, M. Trekels, M.R. da Silva, J.P. Araújo, K. Temst, and A. Vantomme: "Emission channeling studies on a challenging case of impurity lattice

location: cation versus anion substitution in transition-metal doped GaN and ZnO", accepted by Nucl. Instr. Meth. B.

[15] D.J. Silva, U. Wahl, J.G. Correia, and J.P. Araújo: "Influence of the doping on the lattice sites of Fe in Si", Proc. 27th Int. Conf. Defects in Semiconductors (ICDS), Bologna, Italy, 21.-26.7.2013, accepted by AIP Conf. Proc.

[16] B. De Vries, U. Wahl, S. Ruffenach, O. Briot, and A. Vantomme: "Influence of crystal mosaicity on axial channeling effects and lattice site determination of impurities", accepted by Appl. Phys. Lett.

[17] L.M. Amorim, U. Wahl, L.M.C. Pereira, S. Decoster, D.J. Silva, M.R. da Silva, A. Gottberg, J.G. Correia, K. Temst, and A. Vantomme: "Direct measurement of the lattice location of implanted Mg in AlN", to be submitted to Appl. Phys. Lett.

[18] L.M.C. Pereira, U. Wahl, J.G. Correia, L.M. Amorim, D.J. Silva, E. Bosne, S. Decoster, M.R. da Silva, K. Temst, and A. Vantomme: "Cation versus anion substitution by transition metals in GaN and ZnO", to be submitted to Phys. Rev. B.

6b) References:

[19] D.D. Awschalom and R.K. Kawakami: "Teaching magnets new tricks", Nature 408 (2000) 923-924.

[20] A.H. Macdonald, P. Schiffer, and N. Samarth: "Ferromagnetic semiconductors: moving beyond (Ga,Mn)As", Nature Materials 4 (2005) 195-202.

[21] T. Dietl: "A ten-year perspective on dilute magnetic semiconductors and oxides", Nature Materials 9 (2010) 965-974.

[22] L.M.C. Pereira, J.P. Araújo, M.J. Van Bael, K. Temst, and A. Vantomme: "Practical limits for detection of ferromagnetism using highly sensitive magnetometry techniques", J. Phys.D:Appl. Phys. 44 (2011) 215001/1-10.

[23] L.M.C. Pereira, J.P. Araújo, U. Wahl, S. Decoster, M.J. Van Bael , K. Temst, and A. Vantomme: "Searching for room temperature ferromagnetism in transition metal implanted ZnO and GaN", J Appl. Phys. 113 (2013) 023903/1-10.

[24] K.W. Edmonds, P. Bogusławski, K.Y.Wang, R.P. Campion, S.N. Novikov, N.R.S. Farley, B.L. Gallagher, C.T. Foxon, M. Sawicki, T. Dietl, M.B. Nardelli, and J. Bernholc: "Mn Interstitial Diffusion in (Ga;Mn)As", Phys. Rev. Lett. 92 (2004) 037201/1-4.

[25] M. Dobrowolska, K. Tivakornsasithorn, X. Liu, J.K. Furdyna, M. Berciu, K.M. Yu, and W. Walukiewicz: "Controlling the Curie temperature in (Ga,Mn)As through location of the Fermi level within the impurity band", Nature Materials 11 (2012) 444-449.

[26] G.F. Dionne: "Evidence of magnetoelastic spin ordering in dilute magnetic oxides", J. Appl. Phys. 101 (2007) 09C509/1-3.

[27] G.F. Dionne and H.S. Kim: "Magnetostriction effects of $3d^4$ and $3d^6$ ions in dilute magnetic oxide films", J. Appl. Phys. 103 (2008) 07B333/1-3.

[28] D.H. Kim, L. Bi, P. Jiang, G.F. Dionne, and C.A. Ross: "Magnetoelastic effects in $SrTi_{1-x}M_xO_3$ (M = Fe, Co, or Cr) epitaxial thin films", Phys. Rev. B 84 (2011) 014416/1-9.

[29] U. Wahl, J.G. Correia, A.C. Marques, C.P. Marques, E. Alves, L. Pereira, J.P. Araújo, and K. Johnston: "Ion implantation doping of $SrTiO_3$", IAEA Technical Document IAEA-TECDOC-1607 (2008) 43-52.

[30] D.D. Awschalom. L.C. Bassett, A.S. Dzurak, E.L. Hu, and J.R. Petta: "Quantum Spintronics: Engineering and Manipulating Atom-Like Spins in Semiconductors", Science 339 (2013) 1174-1179.

[31] B. Monemar, P.P. Paskov, G. Pozina, C. Hemmingsson, J.P. Bergman, T. Kawashima, H. Amano, I. Akasaki, T. Paskova, S. Figge, D. Hommel, and A. Usui: "Evidence for two Mg related acceptors in GaN", Phys. Rev. Lett. 102 (2009) 235501/1-4.

[32] S. Lany and A. Zunger: "Dual nature of acceptors in GaN and ZnO: The curious case of the shallow Mg_{Ga} deep state", Appl. Phys. Lett. 96 (2010) 142114/1-3.

[33] J.L. Lyons, A. Janotti, and C.G. Van de Walle: "Shallow versus deep nature of Mg acceptors in nitride semiconductors", Phys. Rev. Lett. 108 (2012) 156403/1-4.

[34] S. Garaj, W. Hubbard, and J. A. Golovchenko: "Graphene synthesis by ion implantation", Appl. Phys. Lett. 97 (2010) 183103/1-3.

[35] G. Davies: "The optical properties of luminescence centres in silicon", Physics Reports 176 (1989) 85-188.

[36] A. Docaj and S.K. Estreicher: "Three carbon pairs in Si", Physica B 407 (2012) 2981-2984.

[37] F. Zirkelbach, B. Stritzker, K. Nordlund, J.K.N. Lindner, W.G. Schmidt, and E. Rauls: "Defects in carbon implanted silicon calculated by classical potentials and first-principles methods", Phys. Rev. B 82 (2010) 094110/1-6.

[38] A. Mader, J.D. Meyer, and K. Bethge: "Lattice location of implanted carbon in GaAs", Nucl. Instr. Meth. B 68 (1992) 149-153.

Appendix

DESCRIPTION OF THE PROPOSED EXPERIMENT

The experimental setup comprises:

Part of the Choose an item.	Availability	Design and manufacturing
EC-SLI, on-line emission channeling chamber at GHM	☒ Existing	☒ To be used without any modification
three off-line emission channeling setups currently running in 275 r-011 to be moved into the new laboratory 508.	☒ Existing	☒ To be used without any modification ☐ To be modified
	☐ New	☐ Standard equipment supplied by a manufacturer ☐ CERN/collaboration responsible for the design and/or manufacturing
SSP-GLM implantation chamber	☒ Existing	☒ To be used without any modification ☐ To be modified
	☐ New	☐ Standard equipment supplied by a manufacturer ☐ CERN/collaboration responsible for the design and/or manufacturing
[insert lines if needed]		

HAZARDS GENERATED BY THE EXPERIMENT

(if using fixed installation) Hazards named in the document relevant for the fixed installation. [EC-SLI, On-line Emission Channeling Chamber at GHM + three off-line emission channeling setups currently in 275 r-011 to be moved into the new laboratory 508]

Additional hazards:

Hazards	*EC-SLI Chamber at GHM*	*3 off-line emission channeling setups in 275 r-011 (→508)*	*SSP-GLM implantation chamber*
Thermodynamic and fluidic			
Pressure	[-][Bar], [-][l]	[-][Bar], [-][l]	[-][Bar], [-][l]
Vacuum	10^{-6} mbar, 70 l	10^{-6} mbar, 10-30 l	10^{-6} mbar, 30 l
Temperature	[Room temperature] [K]	[Room temperature] [K]	[Room temperature] [K]
Heat transfer			
Thermal properties of materials	At the sample holder inside the chamber, under vacuum, there is an annealing system up to 1173 K. A closed cycle refrigerator can cool samples down to 50 K	At the sample holder inside the chambers, under vacuum, there is an annealing system up to 1173 K.	
Cryogenic fluid	[He gas], [13][Bar], [3][l] Closed cycle He refrigerator		
Electrical and electromagnetic			
Electricity	[220] [V], [25][A]	[220] [V], [15][A]	
Static electricity			
Magnetic field	[magnetic field] [T]	[magnetic field] [T]	

Batteries	☐	☐	
Capacitors	☐	☐	
Ionizing radiation			
Target material	Solid-state ,single crystal samples for analysis, mounted into a goniometer under vacuum. The short-lived isotopes are directly implanted into the sample and measurements are done in situ.	Solid-state, single crystal samples for analysis, mounted into a goniometer under vacuum. The samples are implanted at the SSP-implantation chamber at ISOLDE – GLM then mounted at the goniometers on each setup and measured under vacuum until their decay.	
Beam particle type (e, p, ions, etc)	Isolde radioactive ion beams		Isolde radioactive ion beams
Beam intensity	From pA to nA		From pA to nA
Beam energy	From 30 to 60 keV		From 30 to 60 keV
Cooling liquids	[liquid]		
Gases	[gas]		
Calibration sources:	☒ calibrations are done on-line with real samples during the runs, or using weak sources implanted with long lived isotopes, e, g, 73 As (80d – c.e. emitter) or 59Fe (44.5d – β-emitter)	☒ calibrations are done on-line with real samples during the measurements or using weak sources implanted with long lived isotopes, e, g, 73 As (80d – c.e. emitter) or 59Fe (44.5d – β-emitter)	
• Open source	☒ 56Mn (2.6 h) *Max activity: 40MBq (5E11 atoms per 3 h shot load)* 61Mn (4.6 s) *Max activity: 250kBq (satur.)* → 61Fe (6 min) → 61Co (1.6 h) *Max activity: 2.5MBq (2E10 atoms per 3 h shot load)* 65Ni (2.5 h) *Max activity: 40MBq (5E11 atoms per 3 h shot load)* 27Mg (9.5 min) *1.2MBq (satur.)* 11Be (13.8 s) *0.8MBq (satur.)* 11C (20 min) *6MBq (satur.)* 11C16O+ molecule	☒ 59Fe (45 d) *Max activity: 90kBq (5E11 atoms* per sample)	☒ 59Fe (45 d) *Max activity: 720kBq (5E11 atoms* per sample, 8 samples max. in chamber)
• Sealed source	☐ [ISO standard]		
• Isotope			
• Activity			
Use of activated material:			
• Description	☐		
• Dose rate on contact and in 10 cm distance	Max. 500 μSv/h at contact at the chamber walls, during experiments, depending on isotope and yield. Typical is ~100 μSv/h on contact. at the chamber walls, ~50 μSv/h in 10 cm distance.	< 50 μ Sv/h at chamber contact	< 200 μ Sv/h at chamber contact The chamber is enclosed by concrete blocks that shield radiation at the working zones to ambient background of the ISOLDE

	The chamber is enclosed by concrete blocks that shield radiation at the working zones to ambient background of the ISOLDE hall, < 5 μSv/h. Experiments are remotely monitored.		hall, < 5 μSv/h.
• Isotope			
• Activity			
Non-ionizing radiation			
Laser			
UV light			
Microwaves (300MHz-30 GHz)			
Radiofrequency (1-300MHz)			
Chemical			
Toxic	[chemical agent], [quantity]		
Harmful	[chemical agent], [quantity]		
CMR (carcinogens, mutagens and substances toxic to reproduction)	[chemical agent], [quantity]		
Corrosive	[chemical agent], [quantity]		
Irritant	[chemical agent], [quantity]		
Flammable	[chemical agent], [quantity]		
Oxidizing	[chemical agent], [quantity]		
Explosiveness	[chemical agent], [quantity]		
Asphyxiant	[chemical agent], [quantity]		
Dangerous for the environment	[chemical agent], [quantity]		
Mechanical			
Physical impact or mechanical energy (moving parts)	[location]		
Mechanical properties (Sharp, rough, slippery)	[location]		
Vibration	[location]		
Vehicles and Means of Transport	[location]		
Noise			
Frequency	[frequency],[Hz]		
Intensity			
Physical			
Confined spaces	[location]		
High workplaces	[location]		
Access to high workplaces	[location]		
Obstructions in passageways	[location]		
Manual handling	[location]		
Poor ergonomics	[location]		

0.1 Hazard identification

3.2 Average electrical power requirements (excluding fixed ISOLDE-installation mentioned above): *(make a rough estimate of the total power consumption of the additional equipment used in the experiment)*

About 5 kW for the on-line chamber at GHM. Each of the 3 off-line setups about 2 kW.